Proceedings of the 4th WSEAS International Conference on Fluid Mechanics and Aerodynamics, Elounda, Greece, August 21-23, 2006 (pp253-261)

Near and far field experimental investigation on the structure of an isothermal lobed jet

I. NASTASE[1], A. MESLEM[1], I.COLDA[2]
[1]Civil and Mechanical Engineering Department
University of La Rochelle
Avenue Michel Crépeau 17042, La Rochelle, Cedex 01
FRANCE
[2]Faculty of Building Services
Technical University of Civil Engineering Bucharest
Bd-ul Pache Protopopescu Nr. 66, Sector 2, cod 73232
ROMANIA

Abstract: - Near and far field experimental research on the structure of an isothermal turbulent lobed jet is presented. Lobed jet mixing performance is compared to an isothermal axisymmetric jet with same equivalent diameter and initial volumetric rate. The entrainment ratio of the lobed jet was found respectively several times greater in the potential core region and 35% greater in the far field than the one of the circular jet. Compared to elliptical or tabbed jets reported by other researchers the lobed jet presents a greater self-induction. The conservation of a greater entrainment rate in the far field turns out to be correlated with a weaker turbulence level. We noticed, as well, that the lobed jet strong dilution by the entrained air does not lead to lower velocity magnitude levels at distant regions. The transformation of the turbulent field by the lobed nozzle geometry enable greater entrainment overall the explored distance range preserving its axial throw. These results suggest that the lobed jet is less dissipative.

Key-Words: - passive flow control, mixing enhancement, jet flow dynamics

1 Introduction

Active and passive control of jet flows has been widely used to improve combustion and to reduce pollutants in mixing chambers and burners. It has been also applied to reduce infrared radiation signal and ejectors noise in military aircraft.

Active methods use controlled excitation of the jet flow which favors under certain conditions the appearance of large scale structures with considerable energy levels that are responsible for mixing (Zaman and Hussain [1], Hussain and Husain [2], Lai [3], Zaman [4], Lin et al.[5]).

Cheaper and easier to apply, passive methods consist in using three-dimensional geometry nozzles. These nozzles became progressively complex in the latest decennials in order to improve self-induction of asymmetrical coherent structures. The earliest studies have been performed on jets issued from rectangular diffusers [6-11] and revealed significant information on the structure and the dynamics of such type of jet flow. An interesting phenomenon was in particular discovered, namely, the jet's major and minor axis switching. Krothapalli et al.[11] proposed a linear dependence between the distance from the nozzle to the first cross-over location and the nozzle aspect ratio. Later, Quinn [12] showed the existence of four pairs of counter rotating streamwise vortices near the exit of the rectangular jet playing a significant role in momentum transport. The same investigator has also reported a distortion of the cross jet geometry from a rectangular shape in the initial region to an elliptic shape in the far field. This is caused by the distortion of the spanwise vortices in addition to the non-uniform self-induction in the shear layer. Large aspect ratio rectangular jets (5 or larger) [6] have not presented significantly greater entrainment than an axisymmetric jet, therefore Ho and Gutmark [13] had the idea of evaluating entrainment rate for a small aspect ratio elliptic jet. Their results were much convincing, showing an entrainment flow rate in the potential core, 3 to 8 times greater than for a circular or a two-dimensional jet. It was also showed that the entrainment is mainly produced in the portion near the minor plane due to the azimuthal distortion phenomenon of the elliptic vortex of Kelvin-Helmholtz. It appears that the aspect ratio has a major influence on the elliptic jet mixing performance knowing that Zaman [14] found for an aspect ratio a/b=3 an entrainment rate hardly superior on that of the circular jet with the same initial Reynolds number. On the other hand, Hussain and Husain [2] showed that elliptic jets unlike circular or plane jets, are characterized by a variation of the turbulent structures azimuthal curvature, leading to a

non uniformity of the self-induction and consequently to a complex three-dimensional distortion that results in axis switching. They also emphasized a shorter potential core compared to a reference circular jet and higher levels of turbulent kinetic energy.

In a continuing effort to increase spreading and mixing performance of jet flows, other various methods have been explored. Rectangular and circular tabbed nozzles have showed particular mixing efficiency compared to the same geometries without mechanical tab intrusions [4],[14-16]. Each tab produces a pair of counter rotating streamwise vortices that modify turbulent structures and increase mixing with ambient flow.

Geometrical manipulation of diffuser nozzles has been subsequently oriented to more complex shapes [17, 18], and it has been suggested in recent work of Hu et al. [19-22], that the lobed nozzle is an extraordinary mixing device. The exploration of the first four equivalent diameters of a lobed jet flow revealed the existence of a pair of large scale streamwise vortices at every lobe peak which dominate spreading and mixing enhancement phenomena. Based on the vorticity field and averaged turbulent kinetic energy profile analysis, they suggest that mixing enhancement of the lobed jet is concentrated in the region of the first two equivalent diameters. Beyond that distance, self-induction level should converge to a rate which is comparable to that of the circular jet.

These observations are promising for the lobed jet mixing performance in the near field. However, a quantification of the entrainment flow rate is missing. Therefore, a comparison with previous cited asymmetric jets could not be done.

The present study could be placed in the continuity of previous work. Its main objective is the characterization of a lobed jet issued from a nozzle with same geometry as Hu et al.[19] by means of two-dimensional Laser Doppler Anemometry. In order to verify the assumption that mixing enhancement is limited on two first equivalent diameters, this investigation will consider greater streamwise distance. This distance was chosen to be about of 20 equivalent diameters.

Beyond lobed jet dynamics within this region, we will particularly discuss characteristics of self-induction phenomenon. Its entrainment rate will be afterwards quantified and compared to a reference circular jet with same initial volumetric flow rate and exit area. It will be also compared to the entrainment rate of the elliptic end tabbed jet which mixing performance has been showed in previous works.

2 Experimental set-up and exit conditions

2.1 Experimental set-up

Turbulent isothermal air jets issued from a circular reference nozzle having the diameter of 40 mm and from a lobed nozzle with the same geometry as the one studied by Hu et al. [19] with the equivalent diameter of 40 mm (Fig. 1) were investigated within an axial distance of $X=20D_e$. The lobe width and height are respectively $\lambda=6$ mm and H=15 mm. The inner and outer lobe penetration angles are $\alpha_{in}=22°$ and $\alpha_{out}=14°$.

Mean velocity fields measurements employed a two-dimensional Laser Doppler Anemometer made by Dantec. The LDA compact system has two solids lasers: one Nd: Yag of 25 mW, providing a monochromatic green beam (514.5 nm) and one Sapphire of 22 mW providing monochromatic blue beam (488 nm).The measuring volume at the laser beams intersection was 0.04×0.045×0.378 mm large. The probe was mounted on a three-dimensional traverse system which enabled the acquisition of two components of the flow velocity, U and V. This three-dimensional traverse has the ranges on the X, Y, Z axis respectively 690 mm, 2020 mm and 690 mm. The air jet flow was seeded with small paraffin oil droplets having the diameter of about 3µm, provided by a liquid seeding generator from Dantec.

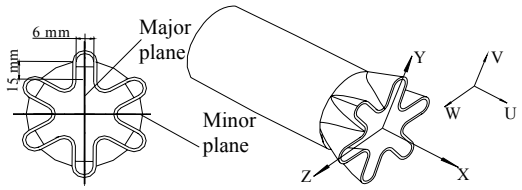

Fig. 1: Lobed nozzle and coordinate system

The air jet experimental facility (showed in Fig. 1) consists of a centrifuge fan connected to a copper pipe having the diameter of 40 mm and the length of 1m. A honeycomb was mounted upstream the nozzle at the end of the pipe, in order to reduce turbulence level at the nozzle exit.

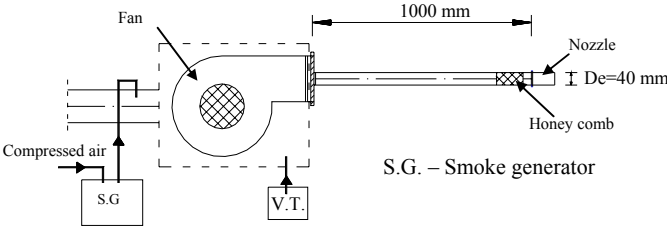

Fig. 2: Plane view sketch of the flow facility

2.2 Exit conditions

Fig.3 shows exit velocity profiles for the two nozzles at an axial distance $X=0.25D_e$. The initial volumetric

flow rate based on the mean velocity field at the nozzle exit was 4.83 10^{-3} m^3/s for the circular jet and 4.70 10^{-3} m^3/s for the lobed jet. This could be traduced by a relative small deviation on the order of 2.7%. All the acquisitions were made with a 60 seconds sampling time. The spatial step in the YZ plane was 2mm.

As it can be observed in Table 1, the lobed jet is accelerated on its exit plane showing a core velocity U_{0C}=5.94m/s. This is to be compared with the circular jet centerline exit velocity U_{0C}=4.88 m/s. The difference between the mean exit velocity and the centerline exit velocity brings us to define two initial Reynolds numbers. The first, noted as $Re_{0,}$ is based on mean exit velocity and it is almost equal for both jets. The second, noted as $Re_{0C,}$ is based on the centerline exit velocity and exhibits different values for the two jets.

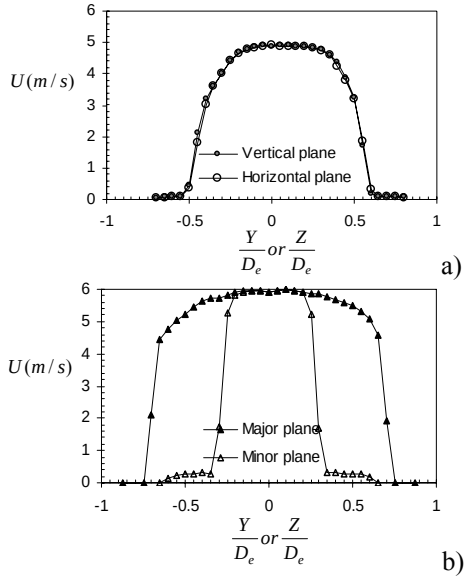

Fig. 3: Exit velocity profiles: a) circular jet, b) lobed jet

Table 1: Exit conditions for the studied jet flows

Nozzle geometry	Q_0 (m^3/s)	U_0 (m/s)	U_{0C} (m/s)	Re_0	Re_{0C}
Circular	4.70 10^{-3}	3.74	5.94	9 520	15 131
Lobed	4.83 10^{-3}	3.84	4.88	9 785	12 453

3 Results and discussion

3.1 Velocity contours and spreading of jet

The spatial distortion and spreading analysis of the lobed jet is first proposed, by means of a comparison with the reference circular jet. In this way, we present in Figs. 4, 5 and 6 the normalized streamwise velocity contours for the lobed and circular jets at different axial distances from the exit plane which vary from X=0.25D_e to X=20D_e. The streamwise velocity was normalized by its mean initial value.

Several interesting phenomena could be observed on these figures. Unlike the lobed jet, the circular jet expands saving its shape which is imposed by the nozzle. It is showed in Fig.4 that the lobe signature, extremely intense at X=0.25De tends to disappear, as noted by Hu et al. [22], at X=3D_e. Further, downstream, at X=5D_e, contour plots become quasi circular. However, compared to the circular jet, its spatial expansion is greater. The geometrical change of the lobed jet conducts to the crossover that could be observed on the momentum thickness and half-velocity width variation (respectively Fig. 7 and Fig.8). A similar phenomenon, namely the switch-over of the major and minor axes, was previously observed for three dimensional jets such as rectangular or elliptic jets ([2], [6, 7], [11], [13, 14]). It has been associated by Hussain and Husain [2] to the dynamics of the azimuthal vortical rings detaching in the shear-layer. For an asymmetric jet the difference of the shear layer curvature is responsible for a non-uniform vortical spanwise velocity distribution which results in sequences of contortions. In certain cases, up to three switchover locations have been observed by Hussain and Husain [2]. In our case, the crossover location for the momentum thickness was situated at X=5D_e and for the half-velocity width at X=3$D_{e.}$ Further downstream it can be observed that the shape of the lobed jet becomes slightly elliptic (Fig.6).

In this second region of the lobed jet it is interesting to notice that momentum thickness and half-jet width in the major plane converge to values of same magnitude as for the circular jet (Figs. 7 and 8). In the minor plane greater values of the momentum thickness and half-jet width are observed and this remains valid until X=20D_e.

3.2 Entrainment flow rate and axial velocity decay

In order to quantify mixing performance for the lobed jet, we have first calculated the volumetric flow rate Q based on the cross plane distribution of the streamwise velocity U for every axial distance X. As a reference, the entrainment rate for the circular jet has been also evaluated at several axial distances.

The different behavior of the lobed jet in the near and far fields enables us to propose a discussion of its self-induction efficiency. This analysis consists of two phases. In the first place, we were interested by the near field (as is showed on Fig. 9) which extends up to five equivalent diameters. On Fig. 9 are also reported available results for circular and asymmetric jets explored by various authors. Experimental conditions and other complementary results are indicated in Table 2. It is to be noticed that the axial variation for the circular jet is quasi linear with a slope of 0.23 within the experimental values of 0.21 and 0.25 found by Zaman [14] and [23].

If we now consider the asymmetric jets in the same region and we perform by a linear approximation of the evolution of the normalized flow rates (Table 2) we could compare values of their slopes. In this way, we obtain for the lobed jet a slope of 0.50 compared with 0.38 for the circular tabbed jet [14], with 0.36 for the 2:1 aspect ratio elliptic jet [13] and with 0.27 for the 3:1 aspect ratio elliptic jet. Consequently, it is quantitatively showed that the lobed jet deserves to be described as an extraordinary mixing device in the near field as suggested by Hu et al.[19].

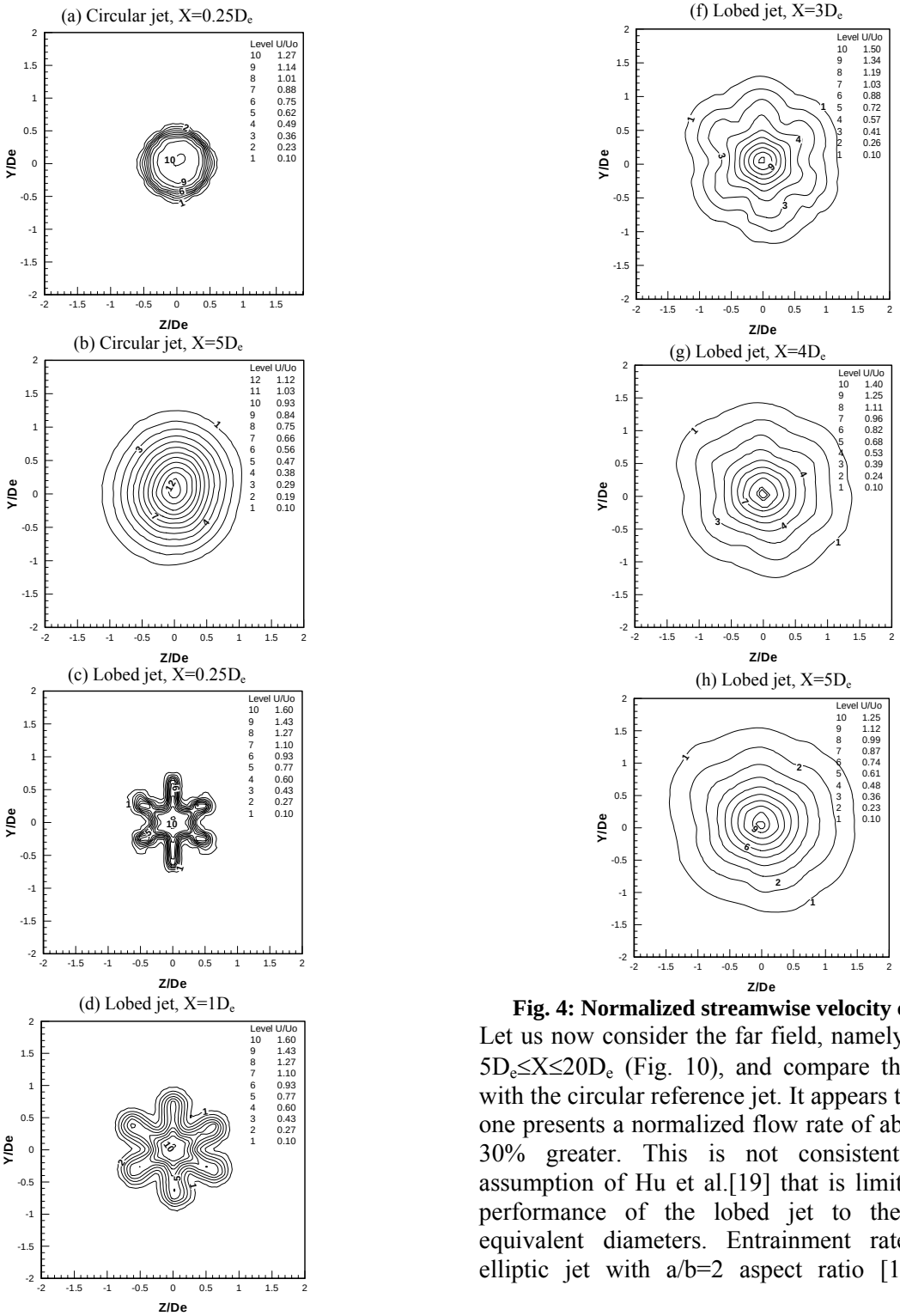

Fig. 4: Normalized streamwise velocity contours

Let us now consider the far field, namely the region $5D_e \leq X \leq 20D_e$ (Fig. 10), and compare the lobed jet with the circular reference jet. It appears that the first one presents a normalized flow rate of about 12% to 30% greater. This is not consistent with the assumption of Hu et al.[19] that is limiting mixing performance of the lobed jet to the first two equivalent diameters. Entrainment rates for the elliptic jet with a/b=2 aspect ratio [13] are not

available beyond $4.5D_e$, so we cannot compare this jet to the lobed jet in the second region.

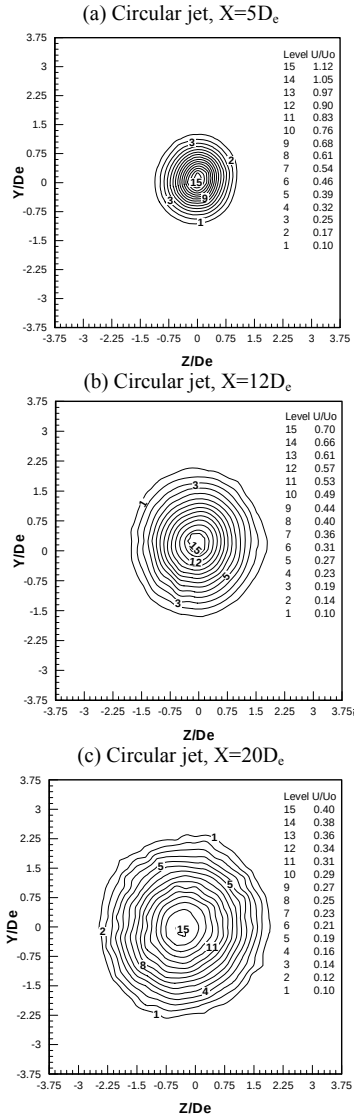

Fig. 5: Normalized streamwise velocity contours for the circular jet

The lobed jet is however compared to the 3:1 aspect ratio elliptic jet and to the tabbed jet investigated by Zaman [14]. Just as like in the first region, the elliptic jet with a/b=3 aspect ratio does not reveal any significant mixing performance. At the opposite, the tabbed jet presents a normalized flow rate comparable with the one of the lobed jet. The initial Reynolds numbers reported by Zaman [14] are 6 to 7 times greater than in the present study (see Table 2).

Considering the influence of this parameter in the behavior of jet flows [24, 25], we take over on Fig.11, the comparison of the mixing performance for asymmetric jets. The entrained flow rate for each asymmetric jet is normalized by the entrained flow rate of the corresponding axisymmetric jet (with same initial Reynolds number).This representation facilitates the appreciation of the lobed nozzle mixing enhancement performance compared to the elliptic and to the circular tabbed nozzles. Although the evolution curve is situated slightly above for the tabbed jet, the strongly decaying slope predicts that the normalized entrainment rate should reach very fast values which are less or equal to 1.

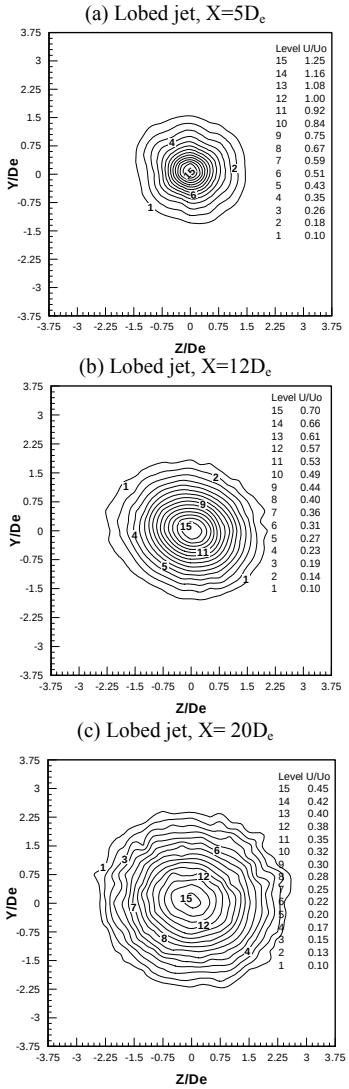

Fig. 6 : Normalized streamwise velocity contours for the lobed jet

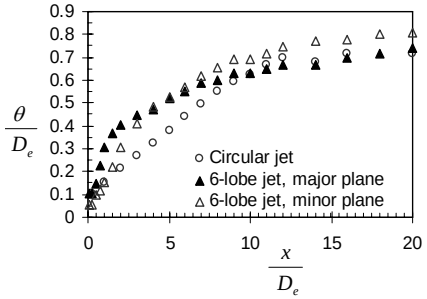

Fig. 7: Variation of momentum thickness

As showed in Table 2, the empirical decay laws of the centerline velocity for the circular and the lobed jet, given by $\frac{U_m}{U_{0C}} = Kv\left(\frac{X + X_0}{D_e}\right)^n$, have same exponents n and very close K_v coefficients. However, their virtual origins X_0 are not the same due to different potential core lengths.

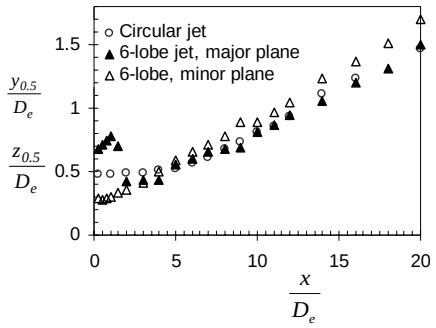

Fig. 8: Variation of velocity half-width

In order to compare the decay of the normalized centerline velocity for the lobed jet and for the asymmetric jets investigated by Zaman [14] we represented in Fig. 13 the streamwise variation of the centerline velocity deviation. This quantity represents the ratio of $\frac{U_m}{U_{0C}}$ values for the asymmetric jet to the corresponding axisymmetric jet. Excepted for the short region within 3 and 8 equivalent diameters, the relative centerline velocity decay of the lobed jet is less rapid compared to the asymmetric jets explored by Zaman [14].

If we limit the analysis to the two of the jets which are offering best mixing performance, namely the lobed jet and the tabbed jet, we can observe that the lobed jet presents the strongest induction and the slowest relative decay of the normalized centerline velocity.

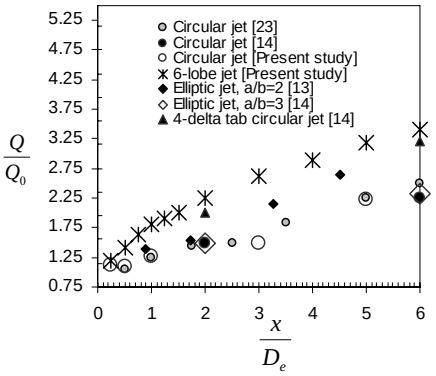

Fig. 9: Near-field volumetric flow rate

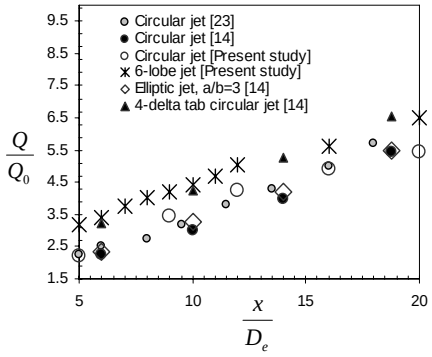

Fig. 10: Far-field volumetric flow rate

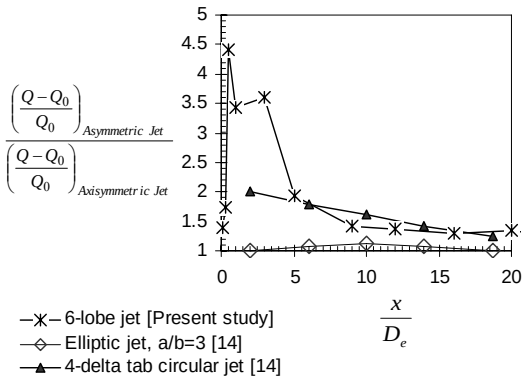

Fig. 11: Normalized entrainment ratio

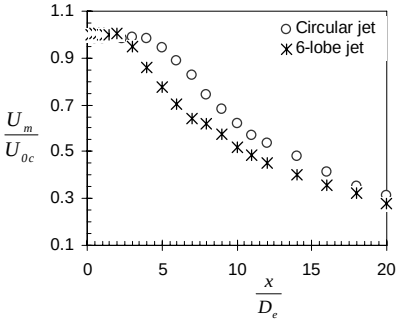

Fig. 12: Variation of centerline velocity

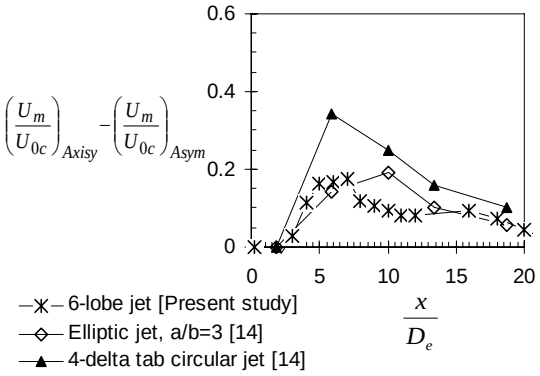

Fig. 13: Relative variation of centreline velocity

3.3 Turbulent structure of the jet

Fig. 14 shows the axial variation of the normalized turbulent momentum flux $\frac{k'}{K_{T0}}$, where K_0 is the total momentum flux at $X=0.25D_e$. Initially, the values of $\frac{k'}{K_{T0}}$ have the same magnitude for both jets, but the evolutions following are different. A steep increase, up to five times the initial level, is observed for the lobed jet within the first equivalent diameter. The peak which is visible here is caused by the intense stirring of the turbulent structures on the borders of the jet. After a slight decrease of $\frac{k'}{K_{T0}}$, it follows a constant evolution up to $X=5D_e$. It is interesting to remark that the value of the turbulent momentum flux in the lobed jet at $X=1D_e$ is not attained in the circular jet before $X=5D_e$.

Table 2: Comparison of the present study with previous works

A	B	C	D	E	F	G	H	I	J	K	L	M	N	O	P	R
Zaman [23]	Circular	$X \leq 22\ D_e$	Air	300 000	-		-	-	0.25	0.991	$0D_e \leq X \leq 5D_e$	-	-	-	-	-
Zaman [14]	Circular	$X \leq 18.75\ D_e$	Air	85 000	-	-	-	-	0.21	0.998	$1D_e \leq X \leq 6D_e$	8.53	$2.20D_e$	-1	0.986	$5.94\ D_e \leq X \leq 18.75\ D_e$
Hu et al. [20]	Circular	$X \leq 4\ D_e$	Water	6 000	-	3%	-	-	-	-	-	-	-	-	-	-
Present study	Circular	$X \leq 20\ D_e$	Air	12 453	9 785	2.5%	-	-	0.23	0.953	$0.25D_e \leq X \leq 5D_e$	6.01	$-0.34\ D_e$	-1	0.993	$9\ D_e < X < 20\ D_e$
Ho and Gutmark [13]	Elliptic (a/b)=2	$X \leq 32\ D_e$	Air	78 000		0.4%	$X = 26.9\ D_e$	$X=3.6D_e$ $X=19.1D_e$ $X = 26.9\ D_e$	0.36	0.992	$0D_e \leq X \leq 4.52D_e$	-	-	-	-	-
Zaman [14]	Elliptic (a/b)=3	$X \leq 18.75\ D_e$	Air	85 000	-	-	-	-	0.27	0.992	$1D_e \leq X \leq 6D_e$	7.51	$3.28D_e$	-1	0.999	$5.94\ D_e \leq X \leq 18.75\ D_e$
Zaman [14]	Circular with delta tabs	$X \leq 18.75\ D_e$	Air	85 000	-	-	-	-	0.38	0.975	$1D_e \leq X \leq 6D_e$	7.23	$2.66D_e$	-1	0.992	$5.94\ D_e \leq X \leq 18.75\ D_e$
Hu et al. [20]	Lobed	$X \leq 4\ D_e$	Water	6 000	-	3%	-	-	-	-	-	-	-	-	-	-
Present study	Lobed	$X \leq 20\ D_e$	Air	15 131	9 520	3.5%	$X=5\ D_e$	$X=3\ D_e$	0.50	0.905	$0.25\ D_e \leq X \leq 5\ D_e$	6.22	$2.26\ D_e$	-1	0.995	$7\ D_e < X < 20\ D_e$

A - Author(s) ;
B - Nozzle geometry;
C - Explored region ;
D - Fluid;
E - Re_{0c} ;
F - Re_0 ;
G - Turbulence level on the nozzle exit;
H - Crossover location of the momentum thickness, θ;
I - Crossover location of the half-jet widths, $Y_{0.5}$ and $Z_{0.5}$;
J - Volumetric entrainment rate, $(D_e/Q_0)(dQ/dX)$;
K - Data fit coefficient of the volumetric entrainment rate error curve, R^2;
L - Validity range of the volumetric entrainment rate law;
M –Velocity decay coefficient, K_V ;
N - Distance of the virtual origin of the jet, X_0 ;
O - Exponent of the centerline velocity decay law, n;
P - Data fit coefficient of the centerline velocity decay error curve, R^2;
R - Validity range of the centerline velocity decay law.

The $\frac{k'}{K_{T0}}$ streamwise evolution for the circular jet is quasi-linear for the first region and it crosses over the lobed jet evolution at $X=4D_e$. After this crossover, turbulent momentum flux levels remain constantly lower in the lobed jet compared to the reference circular jet. The maximal difference of 30% occurs at about ten equivalent diameters. Downstream the difference between the two jets is stabilized around 18% within $X=20D_e$.

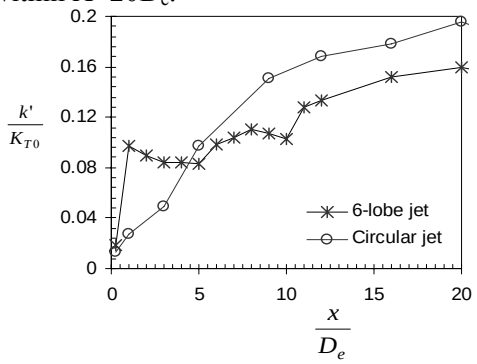

Fig. 14: Streamwise variation of the turbulent momentum flux

To complete this global analysis of the mean turbulent field, we first represented in Fig.15, the centerline variation of the turbulence intensity $\frac{\sqrt{\overline{u'^2}}}{U_{0c}}$.

A peak occurs at $X/D_e=8$ for the circular jet. This is consistent with results of Zaman and Hussain [1] for a circular jet. For the lobed jet the pick occurs earlier, at $X/D_e = 5$. This phenomenon was previously observed by Zaman and Hussain [1] for certain values of the Strouhal number in acoustically excited circular jets. Finally we normalized the RMS of the centerline fluctuation with the local velocity U_m. Three regions can be observed in Fig. 16. The first of them extends up to $X=2D_e$.

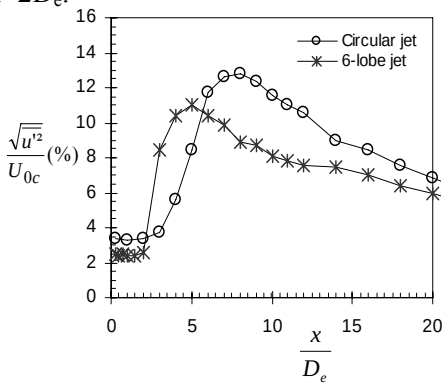

Fig. 15: Centerline variation of the turbulence intensity

At this point the turbulence intensity is weak and has the same magnitude for both of the jets. A second region, for $2D_e<X<7D_e$ reveals a higher turbulence intensity for the lobed jet. At this point the turbulence intensity is weak and has the same magnitude for both of the jets. A second region, for $2D_e<X<7D_e$ reveals a higher turbulence intensity for the lobed jet. This is caused by the coherent asymmetric structures generated by the lobed nozzle which are stirring the flow. In the last region, turbulence intensity for the lobed jet is equal to that of the circular jet at $X=7D_e$ and becomes smaller for $X>7D_e$. This feature was also observed for the plane, circular or elliptic jets under controlled acoustical excitation in a certain range of Strouhal number [3],[26].

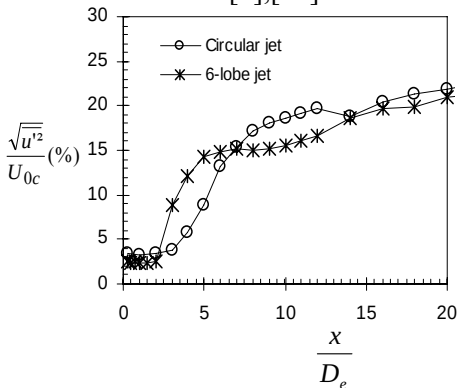

Fig. 16: Turbulence intensity variation along the jet

These results suggest that the lobed jet is less dissipative than the reference circular jet. They also permit to understand the evolution of the normalized centerline streamwise velocity of the lobed jet which converges to that of the circular jet (Fig. 12) in spite of the greater entrainment rate.

4 Conclusion

In this article the results of an experimental study on an isothermal free lobed jet were presented. Dynamic expansion and mixing performance of this jet were analyzed in the near and far fields and compared with a circular reference jet with same initial Reynolds number. In the first region, for $X=5D_e$ the entrained flow rate was found several times greater than for the circular jet. It was also found to be greater than in the case of other asymmetric jets documented in the literature. This strong entrainment is facilitated by the inward and outward penetration angles of the nozzle and it is dominated by coherent structures induced by the asymmetric shape of the nozzle. It is accompanied by an azimuthal distortion of the lobed jet which first becomes circular at the crossover location and afterwards turns in a slightly elliptic shape when axis switches over completely. In the far field, although the mixing performance is much reduced compared to the upstream region, we found that it remains superior to the one of the circular jet, with about 35%. We also showed that the normalized centerline streamwise velocity of the lobed jet converges to same magnitude values as for the circular jet, in spite of its strong entrainment flow rate.

This result is accompanied by a lower turbulence intensity level in the lobed jet compared to the circular reference jet, after an axial distance of about seven equivalent diameters from the exit plane. This

phenomenon of turbulence suppression, already observed for the acoustically excited jets, and the corresponding dynamics brings us to suggest that the lobed jet is less dissipative than the circular jet with same initial Reynolds number.

References:

[1] Zaman K.B. M. Q. and Hussain A. K. M. F. *Vortex pairing in a circular jet under controlled excitation. Part1. General response,* J. Fluid Mech., vol. 101, 1980, part 3, pp. 449-491;

[2] Hussain F. and Husain H.S., *Elliptic jets. Part1. Characteristics of unexcited and excited jets* , J.Fluid Mech., vol. 208, 1989, pp. 257-320 ;

[3] Lai J. C. S., *Turbulence suppression in an elliptic jet* , Int. J. Heat and Fluid Flow, Vol. 13, 1992,No. 1;

[4] Zaman K.B. M. Q., *Axis switching and spreadind of an asymmetric jet: the role of coherent structure dynamics*, J. Fluid Mech., vol. 316, 1996, pp. 1-27;

[5] Lin Y. T., Shieh M. S., Liou H. D. and Hou C. S., *Investigation on the mass entrainment of an acoustically controlled elliptic jet*, Int. Comm. Heat Mass Transfer, Vol. 25, 1998, No. 3, pp. 379-388 ;

[6] Trentacoste N. and Sforza P., *Further experimental results for three-dimensional free jets*, AIAA Journal, Vol. 5, 1967 , pp. 885-891;

[7] Trentacoste N. and Sforza P., *Some remarks on three-dimensional wakes and jets*, AIAA Journal, Vol. 6, 1968, No. 12, pp. 2454-2456;

[8] Sforza, P.M., *A quasi-axisymmetric approximation for turbulent three-dimensional jets and wakes*, AIAA Journal, Vol. 7, 1969, No. 7, pp. 1380-1383;

[9] Sfeir A.A.,*The velocity and temperature fields of rectangular jets* , Int. J. Heat Mass Transfer, Vol. 19, 1976, pp.1289-1297 ;

[10] Sfeir A.A., *Investigation of three-dimensional turbulent rectangular jets*, AIAA Journal, Vol. 17, 1979, No. 10, pp. 1055-1060;

[11] Krothapalli, A., Baganoff, D. and Karamcheti, K., *On the mixing of a rectangular jet* , J. Fluid. Mech., Vol. 107, 1981, pp. 201-220;

[12] Quinn W.R., *Development of a large-aspect-ratio rectangular turbulent free jet* , AIAA Journal , Vol. 32, 1994, No. 3;

[13] Ho C. M. and Gutmark E.J.,*Vortex induction and mass entrainement in a small-aspect–ratio elliptic jet*, J. Fluid Mech., vol. 179, 1987, pp. 383-405 ;

[14] Zaman K.B. M. Q., *Spreading caracteristics and thrust of jets from asymmetric nozzles* , AIAA Paper 96-0200, 1996;

[15] Hu H. Kobayashi T., Wu S. and Shen G., *Changes to the vortical and turbulent structure of jet flows due to mechanical tabs*, Proc. Instn. Mech. Engrs., Vol. 213, 1999, Part C, pp. 321-329, 1999 ;

[16] Hu H., Saga T., Kobayashi T. and Taniguchi N, *Passive control on jet mixing flows by using vortex generators*, Proceedings of the Sixth Triennial International Syposium on Fluid Control, Measurement and Visualisation, Sherbrooke, Canada, August 13-17, 2000 ;

[17] Belovich V. M. and Samimy M., *Mixing processes in a coaxial geometry with a central lobed mixer-nozzle* , AIAA Journal , Vol. 35, No. 5, 1997, pp. 838-841 ;

[18] Yuan Y., *Jet fluid mixing control through manipulation of inviscid flow structures*, Ph.D. Thesis, 2000 Virginia Polytechnic Institute and State University, 262 p.;

[19] Hu H., Kobayashi T., Saga T., Sagawa S. and Taniguchi N, *Particle image velocimetry and planar laser-induced fluorescence measurements on lobed jet mixing flows* , Experimens in Fluids [Suppl.] 2000, S141-S157, Springer Verlag ;

[20] Hu H., Saga T., Kobayashi T. and Taniguchi N, *Research on the vortical and turbulent structures in the lobed jet flow using laser induced fluorescence and particle image velocimetry techniques*, Meas. Sci. Technol., Vol. 11, 2000, pp. 698-711;

[21] Hu H., Saga T., Kobayashi T. and Taniguchi N, *A study on a lobed jet mixing flow by using stereoscopic particle image velocimetry technique*, Physics of fluids, Vol. 13, No. 11, pp. 3425-3441, 2001 ;

[22] Hu H., Saga T., Kobayashi T. and Taniguchi N., *Mixing process in a lobed jet flow* , AIAA Journal, Vol. 40, No. 7, 2002, pp. 1339-1345 ;

[23] Zaman K.B. M. Q., *Flow field and near and far sound field of a subsonic jet*, J. of Sound and Vibration, vol. 106, 1986, pp. 1-16;

[24] Oosthuisen P. H., *An experimental study of low Reynolds number turbulent circular jet flow*, ASME Applied Mechanics, Bioengineering and Fluids Engineering Conference, Houston, U.S.A., paper No. 83, 1983;

[25] Lemieux G. P. and Oosthuizen P. H., *Experimental study of the behavior of plane turbulent jets at low Reynolds numbers* , AIAA Journal, Vol. 23, 1985, No. 12, pp. 1845-1846 ;

[26] Zaman K.B. M. Q. and Hussain A. K. M. F., *Turbulence suppression in free shear flows by controlled excitation*, J. Fluid Mech., vol. 103, 1981 , pp. 133-159;